EUKARYOTIC CELL, July 2009, p. 957–967 Vol. 8, No. 7
1535-9778/09/$08.00+0 doi:10.1128/EC.00251-08

The Cell End Marker Protein TeaC Is Involved in Growth Directionality and Septation in *Aspergillus nidulans*▽†

Yuhei Higashitsuji, Saturnino Herrero, Norio Takeshita, and Reinhard Fischer*

University of Karlsruhe and Karlsruhe Institute of Technology, Institute of Applied Biosciences–Microbiology, Hertzstrasse 16, D-76187 Karlsruhe, Germany

Received 25 July 2008/Accepted 30 April 2009

Polarized growth in filamentous fungi depends on the correct spatial organization of the microtubule (MT) and actin cytoskeleton. In *Schizosaccharomyces pombe* it was shown that the MT cytoskeleton is required for the delivery of so-called cell end marker proteins, e.g., Tea1 and Tea4, to the cell poles. Subsequently, these markers recruit several proteins required for polarized growth, e.g., a formin, which catalyzes actin cable formation. The latest results suggest that this machinery is conserved from fission yeast to *Aspergillus nidulans*. Here, we have characterized TeaC, a putative homologue of Tea4. Sequence identity between TeaC and Tea4 is only 12.5%, but they both share an SH3 domain in the N-terminal region. Deletion of *teaC* affected polarized growth and hyphal directionality. Whereas wild-type hyphae grow straight, hyphae of the mutant grow in a zig-zag way, similar to the hyphae of *teaA* deletion (*tea1*) strains. Some small, anucleate compartments were observed. Overexpression of *teaC* repressed septation and caused abnormal swelling of germinating conidia. In agreement with the two roles in polarized growth and in septation, TeaC localized to hyphal tips and to septa. TeaC interacted with the cell end marker protein TeaA at hyphal tips and with the formin SepA at hyphal tips and at septa.

Filamentous fungi represent fascinating model organisms for studying the establishment and maintenance of cell polarity, because cell growth takes place at the tip of the extremely elongated hyphae. Hyphal extension requires the continuous expansion of the membrane and the cell wall and is driven by continuous fusion of secretion vesicles at the tip (8, 12). The transportation of vesicles is probably achieved by the coordinated action of the MT and the actin cytoskeleton. According to one model, vesicles first travel along MTs, are unloaded close to the hyphal tip, where they form a microscopically visible structure the "Spitzenkörper," which is also called the "vesicle supply center," referring to the assumed function (24, 25). For the last step, vesicle transportation from the Spitzenkörper to the apical membrane, actin-myosin-dependent movement is used. Anti-cytoskeletal drug experiments have shown that hyphae can grow for some time in the absence of MTs but not in the absence of the actin cytoskeleton (14, 27, 30a).

In *Schizosaccharomyces pombe* it was shown clearly that the polarization of the actin cytoskeleton depends on the MT cytoskeleton (2, 7). In 1994, polarity mutants of *S. pombe* were isolated and subsequent cloning of one of the genes identified the polarity determinant Tea1 (19, 29). Because this protein labels the growing cell end, this and other subsequently isolated proteins of this class were named cell end markers. It was shown that cell end localization of Tea1 requires the activity of a kinesin motor protein, Tea2, which transports the protein to the MT plus end (3). Together with the growing MT, Tea1 reaches the cortex, where it is unloaded and binds to a prenylated and membrane-anchored receptor protein, Mod5 (28). The formin For3, which catalyzes actin cable formation, is recruited to the tip through binding to another cell end marker protein, Tea4, which confers tethering to Tea1 (7, 18, 33). Tea4 is required for For3 localization at the cell tip, specifically during initiation of bipolar growth (18).

Recently, it was shown that components of this polarity determination machinery are conserved in the filamentous fungus *A. nidulans* (8). The first component identified was the Tea2 homologue, KipA, a kinesin-7 motor protein (16). Deletion of the gene did not affect hyphal tip extension but polarity determination. Instead of growing straight, hyphae grew in curves. KipA moves along MTs and accumulates at the MT plus end. The identification of Tea1 and a Mod5 homologue was more difficult, because the primary structure of these cell end marker proteins is not well conserved in filamentous fungi. A Tea1 homologue, TeaA, only displayed 27% sequence identity. However, the presence of Kelch repeats in both proteins suggested conserved functions (31). A Mod5 homologue was identified by a conserved CAAX prenylation motif at the C terminus. Systematic analyses of proteins with such a motif in the *A. nidulans* genome led to the identification of TeaR. Like Tea1 and Mod5, TeaA and TeaR localize at or close to the hyphal membrane at the growing cell end (31). However, correct localization of TeaR requires TeaA. In addition, sterol-rich membrane domains define the place of TeaR attachment to the hyphal tip. In contrast to *S. pombe*, TeaA and TeaR are still transported to the hyphal tip in the absence of the motor protein KipA, but their localization is disturbed in comparison to wild type. This suggests that other proteins are necessary for exact TeaA positioning, whose localization depends on KipA.

We characterized a homologue of the *S. pombe* cell end

* Corresponding author. Mailing address: University of Karlsruhe and Karlsruhe Institute of Technology, Institute of Applied Biosciences–Microbiology, Hertzstrasse 16, D-76187 Karlsruhe, Germany. Phone: 49-721-6084630. Fax: 49-721-6084509. E-mail: reinhard.fischer@KIT.edu.

† Supplemental material for this article may be found at http://ec.asm.org/.

▽ Published ahead of print on 8 May 2009.

TABLE 1. *A. nidulans* strains used in this study

Strain[a]	Genotype	Source or reference
TN02A3	*pyrG89*; *argB2* Δ*nkuA*::*argB*; *pyroA4*	22
RMS011	*pabaA1 yA2*; Δ*argB*::*trpC*Δ*B*; *pyroA4*	30
SRL1	Δ*kipA*::*pyr4*; *pyrG89*; *pyroA4* (Δ*kipA*)	16
SJW02	*wA3*; Δ*argB*::*trpC*Δ*B*; *pyroA4*; *alcA(p)*::*GFP*::*tubA* (GFP-MTs)	6
SSK91	SRF200 transformed with pSK76, Δ*teaA*::*argB*; *pyrG89*; Δ*argB*::*trpC*Δ*B*; *pyroA4* (Δ*teaA*)	16
SNT17	*pyrG89*; *wA3*; *alcA(p)*::*GFP*::*kipA-rigor* (GFP-*kipA*-rigor)	31
SNT49	TN02A3 transformed with pNT28 [*teaA(p)-mRFP1-teaA*]	31
SNT28	TN02A3 transformed with pNT9 (*GFP-sepA*)	31
SNT52	SNT49 crossed to RMS011 [*teaA(p)-mRFP1-teaA*]	31
SYH03	TNO2A3 with pYH06 [*alcA(p)-GFP-teaC*]	This study
SYH05	TN02A3 transformed with pYH03 and pYH09 (YFP^N-*sepA* and YFP^C-*teaC*)	This study
SYH06	TN02A3 transformed with pYH01 and pYH09 (YFP^N-*teaA* and YFP^C-*teaC*)	This study
SYH13	SYH03 crossed to SNT52 [*GFP-TeaC*, *teaA(p)-mRFP1-TeaA*]	This study
SYH17	TN02A3 transformed with pYH30 [*teaC(p)-mRFP1-TeaC*]	This study
SYH18	SYH20 crossed to SNT28 [*teaC(p)-mRFP1-TeaC* and *GFP-SepA*]	This study
SYH19	SYH20 crossed to SSK91 [*teaC(p)-mRFP1-TeaC* and Δ*teaA*]	This study
SYH20	SYH17 crossed to RMS011 [*teaC(p)-mRFP1-TeaC*]	This study
SYH21	TN02A3 transformed with pYH14 (Δ*teaC*)	This study
SYH22	SYH20 crossed to SJW02 [*GFP-MT* and *teaC(p)-mRFP1-TeaC*]	This study
SYH23	SYH20 crossed to SNT17 [*GFP-kipA* rigor and *teaC(p)-mRFP1-TeaC*]	This study
SYH24	SYH21 crossed to SNT52 [*teaA(p)-mRFP1-teaA* and Δ*teaC*]	This study
SYH25	SYH17crossed to SRL1 [Δ*kipA* and *teaC(p)-mRFP1-TeaC*]	This study
SYH26	SYH28 crossed to SYH27 (*mRFP1-TeaC* and *GFP-SepA*)	This study
SYH27	TN02A3 transformed with pYH24 (*mRFP1-TeaC*)	This study
SYH28	RMS011 crossed to SNT28 (*GFP-sepA*)	This study

[a] All strains are *veA1*.

marker protein, Tea4, and found that the protein is required for the maintenance of straight polar growth but that it also appears to be involved in septation.

MATERIALS AND METHODS

Strains, plasmids, and culture conditions. Supplemented minimal medium (MM) and complete medium for *A. nidulans* were prepared as described earlier, and the standard strain construction procedures have also been described elsewhere (13). A list of *A. nidulans* strains used in the present study is given in Table 1. Standard laboratory *Escherichia coli* strains (XL1-Blue and Top10F′) were used. Plasmids are listed in Table 2.

Molecular techniques. Standard DNA transformation procedures were used for *A. nidulans* (37) and *E. coli* (26). For PCR experiments, standard protocols were applied using a Biometra TRIO Thermoblock for the reaction cycles. DNA sequencing was done commercially (MWG Biotech, Ebersberg, Germany). Genomic DNA was extracted from *A. nidulans* with the DNeasy plant minikit (Qiagen, Hilden, Germany). DNA analyses (Southern hybridizations) were performed as described previously (26).

Deletion of *teaC*. Flanking regions of *teaC* were amplified by PCR using genomic DNA and the primers TeaC-left-for (5′-GAA CAG TTG CCT TTC GAA AT-3′) and TeaC-left-rev-SfiI (5′-TGG TGG CCA TCT AGG CCG TAG CAG GAT GTT CAA AGG-3′) for the upstream region of *teaC* and the primers TeaC-right-for-SfiI (5-AAT AGG CCT GAG TGG CCC GA CTG GCA CCA CTA C-3′) and TeaC-right-rev (5′-AGA GGC TGG ATT CCT TCT-3′) for the downstream region and cloned into pCR2.1-TOPO to generate plasmids pYH32 and pYH33, respectively. The SfiI restriction sites are underlined. In a three-fragment ligation, the *N. crassa pry-4* gene was released from plasmid pSCI with SfiI and ligated between the two *teaC*-flanking regions, resulting in the vector pYH14.

Transformants of strain TN02A3 were screened by PCR for the homologous integration event. Single integration of the construct was confirmed by Southern blotting (see Fig. S1 in the supplemental material). A total of 20 strains were analyzed, of which 8 showed the *teaC* deletion pattern. All eight deletion strains displayed the same phenotypes. One *teaC* deletion strain was selected for further studies and named SYH21. Coupling of the observed phenotypes with the gene deletion event was confirmed by crosses, recomplementation with *teaC*-derived clones, and downregulation of the gene through the inducible *alcA* promoter.

Tagging of proteins with GFP and mRFP1. To create an N-terminal green fluorescent protein (GFP) fusion construct of TeaC, a 1.2-kb N-terminal fragment of *teaC* (starting from ATG) was amplified from genomic DNA with the primers teaC-AF(5′-TAG GCG CGC CGA TGG CTA GAC CTA GAA TGG-3′) and teaC-PR(5′-CTT AAT TAA TTC TTC AAC AGC CTT AGT TTT-3′) and cloned into pCR2.1-TOPO, yielding pYH34. The restriction sites are underlined. The AscI-PacI fragment from pYH34 was subcloned into the corresponding sites of pCMB17apx, yielding pYH06. To create an N-terminal mRFP1 fusion construct of TeaC, the AscI-PacI fragment from pYH06 was subcloned into the corresponding sites of pDM8, yielding pYH24. To produce TeaC N-terminally tagged with mRFP1 expressed from the native promoter, a 1.5-kb fragment of the *teaC* putative promoter region was amplified from genomic DNA with the primers TeaCp-pro-AvrIII (5′-ACC TAG GTG ACC TTG GGT ATC GTT G-3′) and teaC-pro-KpnI (5′-AGG TAC CAC GAA TTA TGT AGC AGG AT-3′), digested with AvrI and KpnI, and ligated with AvrI-KpnI-digested pYH24, yielding pYH30 (*alcA* promoter replaced with the *teaC* promoter in pYH24). Using the same approach as for TeaC, N-terminal GFP fusion constructs of TeaC were created. All plasmids were transformed into the uracil-auxotrophic strain TN02A3 (Δ*nkuA*). The integration events were confirmed by PCR and Southern blotting (results not shown).

For bimolecular fluorescence complementation (BiFC) analyses, the N-terminal half of YFP (YFP^N) or the C-terminal half of YFP (YFP^C) was fused to the N terminus of the protein of interest. YFP^N (154 amino acids of YFP and 5 amino acids linker) was amplified with the primers fwd-Kpn-YFP-N (5′-CGG TAC CAT GGT GAG CAA GGG CGA GGA GCT G-3′) and rev-YFP-N-Li-Asc (5-CGG CGC GCC CGT GGC GAT GGA GCG CAT GAT ATA GAC GTT GTG GCT GTT GTA G-3′). YFP^C (86 amino acids of YFP and 17 amino acids linker) was amplified with the primers fwd-Kpn-YFP-C (5′-CGG TAC CAT GGC CGA CAA GCA GAA GAA CGG CAT CAA GG-3′) and ev_YFP-C_Li_Asc (5′-CGGCGCGCCGTGGTTCATGACCTTCTGTTTCAGGTCGT TCGGGATCTTGCAGGCCGGGCGCTTGTACAGCTCGTCCATGCCGAG AGTGATCCC-3′). The KpnI-AscI fragment of YFP^N or YFP^C was ligated into KpnI- and AscI-digested pCMB17apx, yielding pDV7 (GFP replaced with YFP^N in pCMB17apx) and pDV8 (GFP replaced with YFP^C in pCMB17apx). To create an N-terminal YFP^C fusion construct of TeaC, the AscI-PacI fragment from pYH06 was subcloned into the corresponding sites of pDV8, yielding pYH08. To create N-terminal YFP^N fusion constructs *teaA* and *sepA* fragments from pNT1, pNT9, were subcloned into the corresponding sites of pDV7, yielding pYH01 and pYH03.

Yeast two-hybrid analysis. The yeast two-hybrid analysis was performed by using the MatchMaker3 Gal4 two-hybrid system (BD Clontech). For bait generation, fragments of *teaC* cDNA corresponding to the N-terminal half of TeaC

TABLE 2. Plasmids used in this study

Plasmid	Construction	Source or reference
pCR2.1-TOPO	Cloning vector	Invitrogen (NV Leek, The Netherlands)
pCMB17apx	*alcA(p)*::*GFP*, for N-terminal fusion of GFP to proteins of interest; contains *N. crassa pyr4*	5
pDM8	GFP replaced mRFP1 in pCMB17apx	34
pSCI	*pry4* with SfiI sites	16
pNT33	N-terminal half of *teaA* cDNA in pGADT7	31
pNT34	N-terminal half of *teaA* cDNA in pGABKT7	31
pNT35	C-terminal half of *teaA* cDNA in pGADT7	31
pSH19	C-terminal half of *teaA* cDNA in pGABKT7	31
pNT6	0.7-kb *teaA* fragment in pDBM8	31
pNT28	1.5-kb *teaA(p)* fragment in pNT6	31
pNT6	0.7-kb *teaA* fragument from pNT1 inpDM8	31
pNT9	1.2-kb *sepA* fragment in pCMB17apx	31
pDV7	GFP replaced N-terminal half of YFP in pCMB17apx	31
pDV8	GFP replaced C-terminal half of YFP in pCMB17apx	31
pYH01	0.7-kb *teaA* fragment from pNT1 in pDV7	31
pYH03	1.2-kb *sepA* fragment from pNT9 in pDV7	31
pYH06	1.2-kb *teaC* fragment in pCMB17apx	This study
pYH08	1.2-kb *teaC* fragment from pYH06 in pDV8	This study
pYH14	*teaC* deletion construct: flanking regions from pYH33 and pYH34 ligated with *pry4* from pCS1	This study
pYH16	N-terminal half of *teaC* cDNA in pGADT7	This study
pYH17	N-terminal half of *teaC* cDNA in pGBK T7	This study
pYH18	C-terminal half of *teaC* cDNA in pGADT7	This study
pYH19	C-terminal half of *teaC* cDNA in pGBKT7	This study
pYH24	1.2-kb *teaC* fragment in pDM8	This study
pYH30	1.5-kb *teaC(p)* fragment in pYH24	This study
pYH32	1.0-kb 5′-flanking region of *teaC* with SfiI site in pCR2.1-TOPO	This study
pYH33	1.0-kb 3′-flanking region of *teaC* with SfiI site in pCR2.1-TOPO	This study
pYH34	1.2-kb *teaC* fragment in pCR2.1-TOPO	This study

(356 amino acids) with the primers TeaC-EF (5′-GGC CGA ATT CAT GGC TAG ACC TAG AAT GG-3′) and TeaC-BMR (5′-GGA TCC TTA CAG TAG GTT CGG AGT GAG-3′) or corresponding to the C-terminal half of TeaC (428 amino acids) with the primers TeaC-EMF (5′-GAA TTC GAA AAG CCG CGC TCA AG-3′) and TeaC-BR (5′-GGC CGG ATC CTT ATT GAC TCG TCG ACC TG-3′) were amplified and cloned into the pGBK7 vector, which contains the Gal4 DNA-BD and the *TRP1* marker, yielding pYH17 and pYH19 (BD Clontech). The fragments of *teaC* cDNA corresponding to the N-terminal half and C-terminal half of TeaC from pYH17 and pYH19 were amplified and cloned into the pGADT7 vector, which contains the GAL4 DNA-AD and the *LEU2* marker (BD Clontech), yielding pYH16 and pYH18. pGBK7-associated plasmids were transformed into yeast Y187 (mating type *MAT*α), and pGADT7-associated plasmids were transformed into yeast AH109 (mating type *MAT***a**). The system utilizes two reporter genes (*HIS3* and *lacZ*) under the control of the GAL4-responsive UAS. The β-galactosidase activity was analyzed by liquid culture assays using ONPG (*o*-nitrophenyl-β-D-galactopyranoside; Sigma) as a substrate. The activity was calculated in Miller units (20). Experiments were repeated three times.

Light and fluorescence microscopy. For live-cell imaging of germlings and young hyphae, cells were grown on coverslips in 0.5 ml of MM plus 2% glycerol (derepression of the *alcA* promoter and thus moderate expression of the gene), MM plus 2% threonine (activation of the gene thus high expression levels), or MM plus 2% glucose (repression of the *alcA* promoter). Cells were incubated at room temperature for 1 to 2 days. For pictures of young hyphae of each gene deletion strain, the spores were inoculated on microscope slides coated with MM plus 2% glucose plus 0.8% agarose and grown at 30°C for 1 day. Images were captured at room temperature by using an Axioimager microscope (Zeiss, Jena, Germany). Images were collected and analyzed by using the AxioVision system (Zeiss).

FM4-64, Hoechst 33342, calcofluor white, benomyl, and cytochalasin A treatment. FM4-64 was used at a concentration of 10 μM in the medium. Coverslips were incubated for 5 min and washed. Benomyl [methyl 1-(butylcarbamoyl)-2-benzimidazole carbamate; Aldrich] was used at a final concentration of 2.5 μg/ml in the medium from a stock solution of 1 mg/ml in ethanol. Cytochalasin A (Sigma) was used at a final concentration of 2 μg/ml in the medium from a stock solution of 100 mg/ml in dimethyl sulfoxide. Calcofluor white was used at a final concentration of 60 μg/ml in the medium. Hoechst 33342 (Molecular Probes) used at a final concentration of 10 μg/ml in the medium.

Protein extracts and Western blotting. For induction of the *alcA* promoter, *A. nidulans* cultures ware shaken in MM containing 2% threonine or 2% glycerol for 48 h. The mycelium was harvested by filtration through Miracloth (Calbiochem, Heidelberg, Germany), dried by pressing between paper towels, and immediately frozen in liquid nitrogen. After the mycelium was ground in liquid nitrogen, the material was resuspended in protein extraction buffer (50 mM Tris-HCl [pH 8], 150 mM NaCl) supplemented with protease inhibitors (1 mM phenylmethylsulfonyl fluoride, 10 μM leupeptin, 1 μM pepstatin). Protein extracts ware clarified twice by centrifugation (centrifuge 5403; Eppendorf, Hamburg, Germany) at 13,000 rpm at 4°C for 10 min. The protein concentration was quantified with a Roti-Quant kit (Roth, Karlsruhe, Germany). After denaturation of the samples, protein extracts were loaded on a 7.5% sodium dodecyl sulfate-polyacrylamide gel. For blotting, nitrocellulose membranes from Schleicher & Schuell (Dassel, Germany) were used. For Western blotting, we used rabbit polyclonal anti-GFP (Sigma-Aldrich, Munich, Germany) at a dilution of 1:4,000 and polyclonal anti-rabbit antibodies coupled to peroxidase (product A0545; Sigma-Aldrich) at a dilution of 1:4,000.

RESULTS

Isolation and deletion of *teaC*. We searched the *A. nidulans* genome at the Broad Institute (Cambridge, MA) (http://www.broad.mit.edu/annotation/genome/aspergillus_group/MultiHome.html) for proteins with similarity to the cell end marker protein Tea4 from *S. pombe* and identified one open reading frame (AN1099.3) (11). DNA and cDNA sequences were confirmed, and five introns with lengths of 66, 60, 66, 46, and 45 bp were determined. We named the gene *teaC*, although sequence similarity between the 687-amino-acid *A. nidulans* protein and the 810-amino-acid *S. pombe* protein

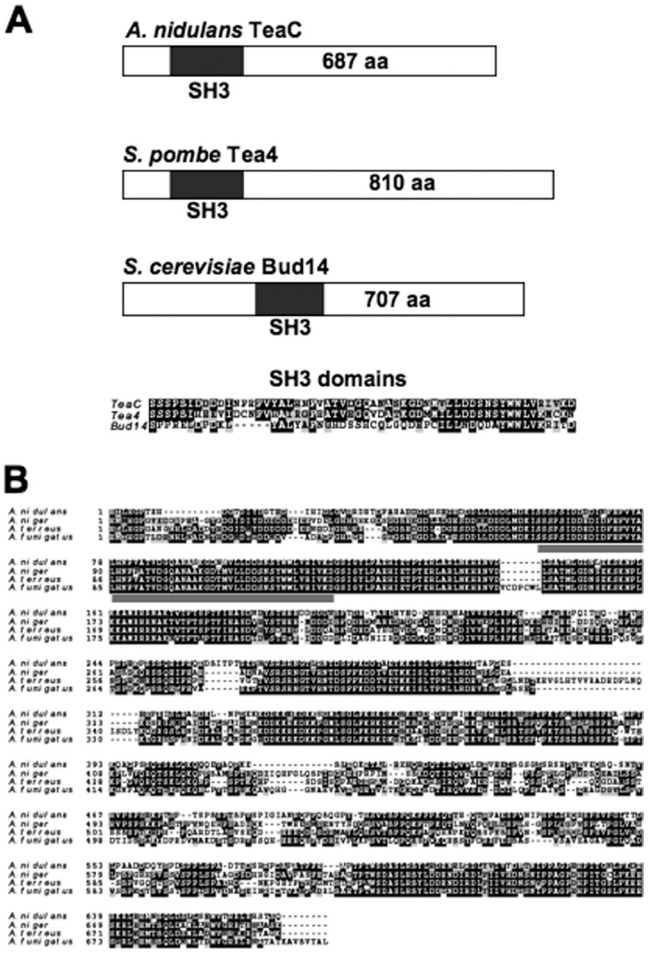

FIG. 1. Comparison of TeaC with related proteins from other fungi. (A) Scheme of *A. nidulans* TeaC, *S. pombe* Tea4, and *S. cerevisiae* Bud14, indicating the location of the SH3 domain. The alignment of the three SH3 domains is displayed below the scheme. (B) Alignment of TeaC homologues from four *Aspergillus* species as indicated. The SH3 domain is highlighted with the red line below the sequences. The alignments were done with CLUSTAL W with standard parameters. Identical amino acids are shaded in black, and chemically conserved amino acids are shaded in gray using the program box shade. aa, amino acids.

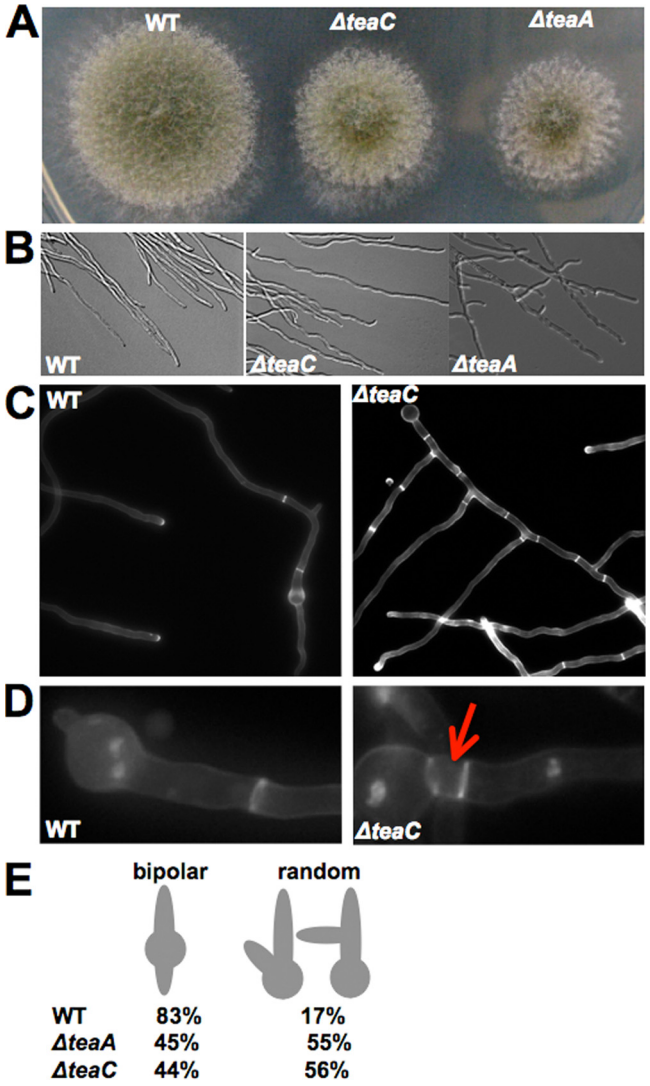

FIG. 2. Phenotypic comparison of wild-type with Δ*teaC* and Δ*teaA* strains. (A) Colonies of wild-type (TN02A3), Δ*teaA* (SSK91), and Δ*teaC* (SYH21) strains. Strains were grown on MM glucose agar plates for 2 days. (B) Hyphae of wild-type, Δ*teaA*, and Δ*teaC* strains were grown for 1 day on microscope slides coated with MM with 2% glucose and 0.8% agarose. Images were taken with differential interference contrast. Hyphae are 3 to 4 μm in diameter. (C) Z-stack image of wild-type (TN02A3) and Δ*teaC* (SYH21) strains grown on MM with 2% glucose for 1 day and stained with calcofluor white. (D) Z-stack image of wild-type (TN02A3) and Δ*teaC* (SYH21) strains grown on glucose MM and stained with calcofluor white and Hoechst 33343. The arrow points to a short, anucleate hyphal compartment. Hyphae are 3 to 4 μm in diameter. (E) Quantification of the effect of different gene deletions on second germ tube formation. Conidia of each strain were germinated in MM with glucose and analyzed for the emergence of the second germ tube. For each strain, 100 germlings were counted. WT, wild type.

was restricted to a conserved SH3 domain (Fig. 1A). Within this 86-amino-acid domain the identity was 63% with an e-value of 6e−27. Outside this region, the homology was very low, and the overall identity was only 12.5%. The sequence similarity to the *S. cerevisiae* Bud14 protein, which shares some functional relationship with Tea4, was even lower. In other aspergilli, proteins with high identities to *A. nidulans* TeaC were found (Fig. 1B). The identity to corresponding proteins from other ascomycetous fungi was again much lower, e.g., *Penicillium chrysogenum* (43%) and *Magnaporthe grisea* (only 22%). Sequence identity to basidiomycetous species was less than 10%. These results indicate that TeaC sequences are only poorly conserved within fungi.

To analyze the function of *teaC* in *A. nidulans*, we constructed a *teaC* deletion strain (SYH21; see Materials and Methods) and compared it to a Δ*teaA* deletion strain constructed previously (31). Both strains produced compact and small colonies (75 to 85% of the diameter) compared to the wild type. The growth defect was slightly more severe in the Δ*teaA* deletion strain (Fig. 2A). In both strains hyphae displayed a zig-zag growth phenotype compared to straight hyphae in the wild type (Fig. 2B). The effect on the maintenance

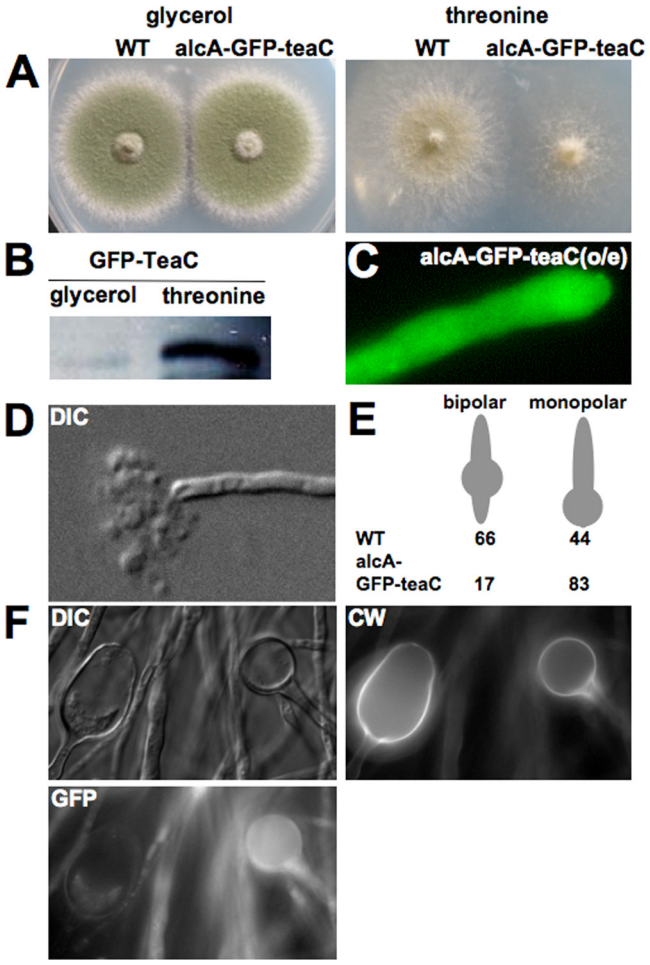

FIG. 3. Effect of overexpression of *teaC*. (A) Comparison of colonies of SYH03 [*alcA(p)-GFP-teaC*] and wild-type strains on glycerol- or threonine-containing medium after 4 days of growth at 37°C. (B) Western blot of hyphae of SYH03 grown on MM with glycerol or threonine as a carbon source. Portions (10 μg) of total protein extract were loaded onto the gel and processed for the Western blot as described in Materials and Methods. (C) Fluorescence microscopic picture of a hypha of SYH03 after induction with threonine for 1 day. (D) Germinated conidia of SYH03 grown on MM with threonine as a carbon source for 48 h observed using differential interference contrast. The hyphal tip had lysed. (E) Quantification of the effect of *teaC* overexpression on the emergence of the second germ tube. For each strain, 100 germlings were counted. (F) Germinated conidia of SYH03 grown on MM with threonine as carbon source for 48 h observed using differential interference contrast, stained with calcofluor white (CW), or observed in the GFP channel. WT, wild type; DIC, differential interference contrast.

of growth directionality was also stronger in the Δ*teaA* strain. The mutant phenotype was mainly seen in germlings.

The Δ*teaC* mutants also showed an increased number of septa and branches, probably due to the reduced extension rate of the hyphae and not specific for the *teaC* deletion (Fig. 2C and see Fig. S2 in the supplemental material). In addition, we noticed some small compartments (5 μm; 8% [$n = 100$]), which did not contain any nucleus (Fig. 2D). This did not occur in the wild type or in slower-growing *A. nidulans* strains.

Another polarity defect has been detected in the way the second germ tube emerges from a conidiospore. In the wild type, the second hypha emerges opposite to the first germ tube (bipolar) in 83% of the spores. In contrast, the second hyphae emerged at random positions in 56% of the spores in the Δ*teaC* mutant strain. A similar defect was observed in 55% of the spores in the Δ*teaA* mutant ($n = 100$) (Fig. 2E). This suggests that *teaA* and *teaC* are required for the selection of the site of polarity initiation.

Overexpression of TeaC inhibits septum formation. We next tested whether overexpression of TeaC would also cause any morphological phenotype. We expressed *teaC* using the control of the *alcA* promoter under inducing conditions (threonine; see Materials and Methods). When the GFP-TeaC strain was grown on threonine MM colonies appeared smaller than the ones from wild type (Fig. 3A). The high expression level of TeaC was shown by Western blotting and an increase in GFP fluorescence (Fig. 3B and C; see also below). Under inducing conditions, we often observed lysis at the hyphal tips (Fig. 3D) and rarely branching of hyphae. Furthermore, the number of conidia that produced a second germ tube was reduced from 66% to 17% ($n = 100$) (Fig. 3E). Some conidia without a second germ tube grew continuously isotropic up to 20 μm in diameter after 2 days. Some hyphae appeared to be empty, probably because of leakage of the cytoplasm. This was visualized by calcofluor white staining of the cell wall and GFP staining of the cytoplasm. Whereas the spore on the right side in Fig. 3F showed fluorescence in both channels, the left spore showed only fluorescence of the cell wall, indicating an empty spore.

When we analyzed the number of septa, we found that *teaC* overexpression repressed almost completely septation (Fig. 4A). Because TeaC interacts with SepA and possibly regulates the localization and/or the activity (see below), we sought to determine which phenotype would be caused by overexpression of TeaC, together with the overexpression of SepA. The displayed phenotype was similar to the phenotype of *teaC* overexpression, namely, very few septa (Fig. 4B and C). In addition, conidia were swollen, hyphae had an irregular shape, and hyphal tips appeared very large. To quantify this effect, we counted the number of septa in germlings, which were between 100 and 300 μm in length ($n = 50$) (Fig. 4C). Overexpression of SepA alone did not cause a reduction of the number of septa, and the morphology was less severely affected (data not shown).

Localization of TeaC at the hyphal tip depends on microtubules (MTs) but not on the kinesin KipA. To investigate the subcellular localization of TeaC, we constructed an *A. nidulans* strain expressing a GFP-TeaC fusion protein under the control of the *alcA* promoter (see above and Materials and Methods). The construct was transformed into strain TN02A3, and a transformant was selected in which the construct was integrated into the *teaC* locus (SYH03). This leads to duplication of the 5′ end of the gene under the control of the endogenous promoter and the *GFP-teaC* fusion construct under the control of the *alcA* promoter. Under repressing conditions, the strain displayed the Δ*teaC* deletion phenotype (see above). Under derepressed conditions, wild-type hyphal morphology was obtained. This experiment showed that the observed phenotypes in the Δ*teaC* deletion strain were indeed caused by the deletion and not by another mutation, and it showed that the GFP-TeaC fusion protein was functional. GFP-TeaC localized to

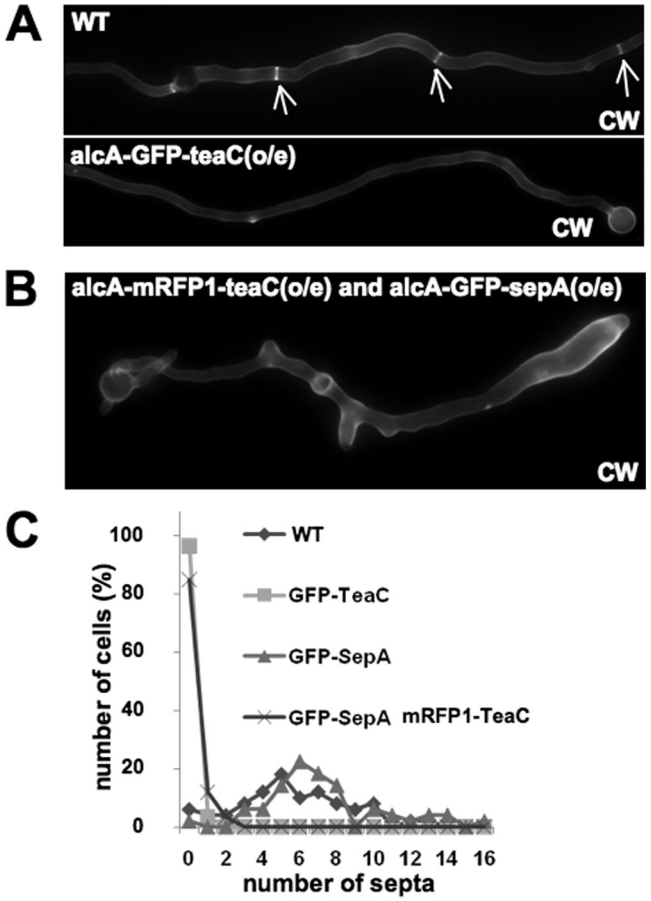

FIG. 4. Effect of overexpression of *teaC* on septation. (A) Strains SYH17 [*teaC(p)-mRFP1-teaC*] (WT) and SYH03 [*alcA(p)-GFP-teaC*] grown on threonine MM and stained with calcofluor white. The red arrows point to the stained septa. Hyphae are 3 to 4 μm in diameter. (B) Strain SYH26 [*alcA(p)-GFP-sepA* and *alcA(p)-mRFP1-teaC*] grown on MM with threonine as carbon source for 48 h and stained with calcofluor white. The ringlike structure is a small branch observed from the top. (C) Quantification of the number of septa in strains SYH17 (considered as the wild type), SYH03, SNT28 [*alcA(p)-GFP-sepA*], and SYH26 grown in threonine MM. A total of 50 germlings were counted for each strain. WT, wild type; CW, calcofluor white.

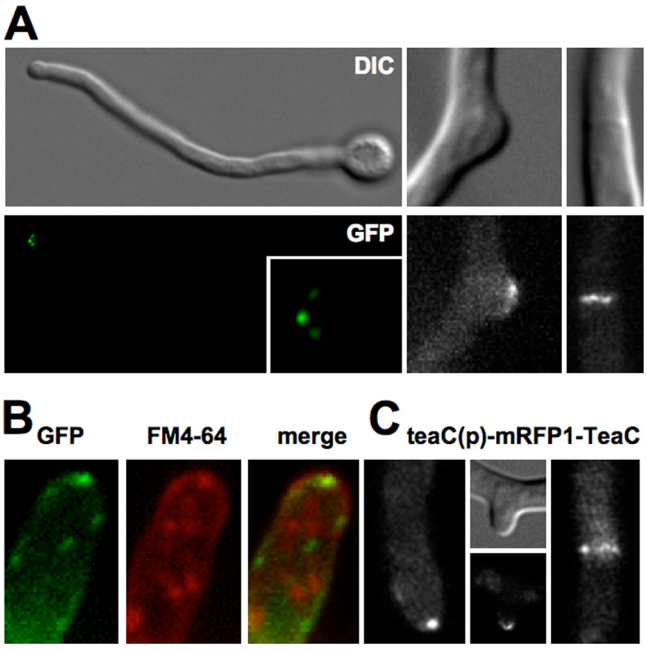

FIG. 5. TeaC localization. (A) Hyphae of strain SYH03 [*alcA(p)-GFP-teaC*] grown on MM with glycerol as a carbon source. The upper row shows differential interference contrast (DIC) pictures; the lower row shows same hyphae in the GFP channel. GFP-TeaC localized to one point in the hyphal apex (enlarged in the inset), at the branching site, and at the septa. (B) Localization of TeaC (GFP) and the Spitzenkörper (visualized with FM4-64). (C) mRFP1-TeaC expressed under the control of the native promoter (SYH17). Fluorescence signals were observed at the hyphal tip and new branches and at the septa. Hyphae are 3 to 4 μm in diameter.

one bright point at all hyphal tips and at newly forming septa (Fig. 5A). In addition, some weaker points on the side of the tip were observed. The GFP-TeaC points always localized close to the plasma membrane or appeared attached to it. Furthermore, some spots appeared in the cytoplasm, which could represent the MT plus ends (see also Fig. 6A).

In growing tips, the Spitzenkörper has an important role as vesicle supply center. To compare the localization of TeaC with the Spitzenkörper, we stained hyphae with FM4-64, which has been used in several fungi to stain the Spitzenkörper (9, 23, 31). The Spitzenkörper appeared to colocalize with GFP-TeaC (Fig. 5B), although from these pictures it was not unambiguously clear whether TeaC is part of the Spitzenkörper or only attached to the membrane and therefore very close to the Spitzenkörper.

To confirm TeaC localization and to prove that the observed localization was not an artifact of the expression under *alcA* promoter control, we constructed a strain (SYH17) producing mRFP1-TeaC under the control of the native promoter. SYH17, in which mRFP1-TeaC is the only source of TeaC, did not show the phenotype observed in the Δ*teaC* mutant, indicating that mRFP1-TeaC at this expression level was also biologically functional. Although signals of mRFP1 appeared much weaker, mRFP1-TeaC still localized to one point, and weaker signals were observed along the apex and at forming septa (Fig. 5C). The single spot of mRFP1-TeaC normally localized at the center of the hyphal apex (Table 3). At a small number of tips (13%, $n = 100$), mRFP1-TeaC localized along the tip membrane. For further experiments, we normally used strains producing mRFP1-TeaC under the native promoter, when we analyzed the localization of TeaC.

To test whether TeaC localization at the hyphal tip depends on MTs, we studied a strain with GFP-labeled α-tubulin and mRFP1-TeaC (SYH22) and found that TeaC localized to the plus end of the MTs, although the signal intensity was close to the detection limit (Fig. 6A). Next, we used the MT-destabilizing drug benomyl. After this treatment (2.5 μg of benomyl/ml), almost all fluorescence of GFP-MTs was diffused into the cytoplasm within 5 min (data not shown), and the mRFP1-TeaC point at the tips was sometimes divided into several points and disappeared after 30 to 40 min from >80% of the tips ($n = 100$) (Fig. 6B and Table 3). The delay between the disappearance of the TeaC spot and the disassembly of the MTs suggests that TeaC is rather stable at the cortex.

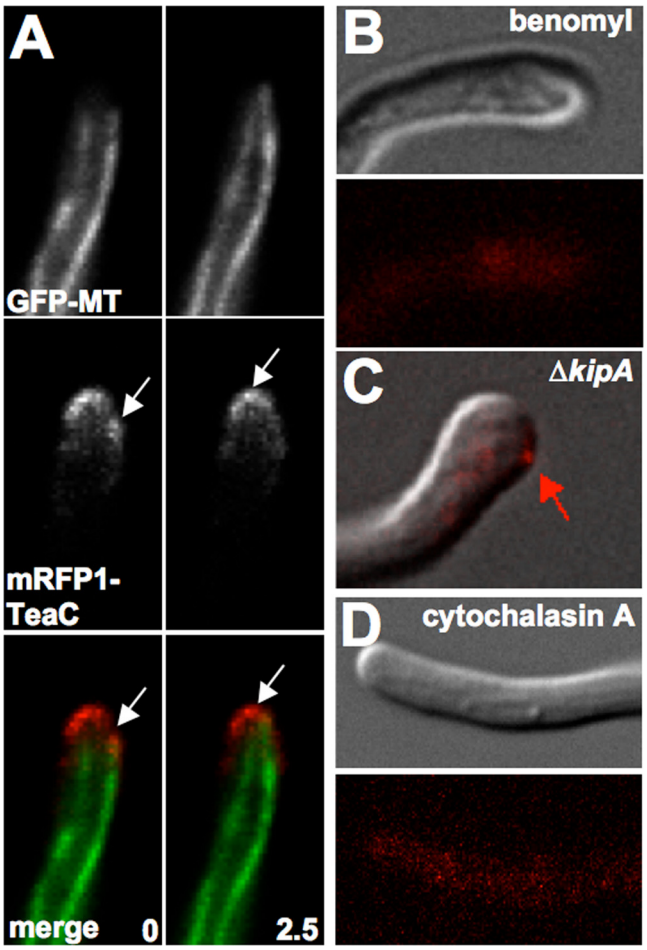

FIG. 6. Relationship between TeaC and MTs. (A) Observation of GFP-labeled MTs and mRFP1-labeled TeaC (SYH22). The arrows point to the MT plus ends. The same hyphae was observed at time zero and after 2.5 s, as indicated in the images. (B) Effect of benomyl on the localization of TeaC in strain SYH22 [*teaC(p)-mRFP1-teaC*]. *A. nidulans* was grown in MM with glycerol for 1 day and then shifted to medium containing 2.5 μg of benomyl/ml for 30 min. (C) In the Δ*kipA* mutant SYH25 TeaC moved away from the center of the apex to the side of the tip (arrow). (D) Effect of cytochalasin A on TeaC localization. SYH17 was grown in MM with glycerol for 1 day and shifted to medium containing 2 μg of cytochalasin A/ml for 2 min. Hyphae are 3 to 4 μm in diameter.

To analyze whether TeaC is transported in a kinesin-7-dependent way to the MT plus end, we studied TeaC localization in a Δ*kipA* mutant. mRFP1-TeaC still localized to one point at nearly 80% of the tips ($n = 100$), indicating KipA-independent polarization. However, the mRFP1-TeaC point did not localize to the center of the apex and moved away to the side of the hypha (Fig. 6C and Table 3). We further studied this effect by localization of TeaC in a KipA^{rigor} mutant, in which KipA (fused to GFP) harbors a point mutation in the ATP-binding domain (16, 38). GFP-KipA^{rigor} binds but does not move along MTs, and thus decorates them. In this strain (SYH23) mRFP1-TeaC still localized at 90% of the tips, but the mRFP1-TeaA point often moved away to the side of the apex and sometimes divided into two points (Table 3). These results indicate that TeaC can be transported independently of KipA to the tip and that other KipA-transported proteins are probably required for exact positioning of TeaC. We are assuming that the key for further understanding of the cell end marker protein complex lies in the characterization of cargoes of the KipA motor protein.

We investigated also the effect of cytochalasin A (2 μg/ml), an inhibitor of actin polymerization, on TeaC localization. mRFP1-TeaC dispersed around the tips within 50% of the tips ($n = 100$) by 2 to 10 min after the treatment (Fig. 6D and Table 3) compared to the control strain only treated with 0.02% dimethyl sulfoxide. Taken together, our results suggest that TeaC localization depends on the MT and the actin cytoskeleton.

TeaC connects TeaA and SepA. To investigate whether *A. nidulans* TeaC colocalizes with TeaA, we constructed a strain (SYH13) expressing mRFP1-TeaA and GFP-TeaC and compared their localization patterns. The mRFP1-TeaA point at the apex colocalized with that of GFP-TeaC. If mRFP1-TeaA localized at two points (10%, $n = 100$) TeaC also colocalized to the same spots (Fig. 7A). Likewise, we tested colocalization of TeaC with SepA. We constructed a strain (SYH18) expressing GFP-SepA and *teaC(p)-mRFP1-teaC*. TeaC and SepA did not obviously colocalize at the hyphal apex. When SepA localized at the hyphal apex, TeaC appeared adjacent to the SepA signal (11%, $n = 100$). When TeaC localized at the hyphal apex at one point, SepA did not localize at the hyphal apex (89%, $n = 100$) (Fig. 7B).

We also found no obvious colocalization at septa (Fig. 7C). It appeared that TeaC surrounded SepA (Fig. 7C). While doing time course experiments, we found that SepA and TeaC follow a constricting ring but that TeaC constriction was slightly delayed in comparison to SepA (Fig. 7D and E).

Next, we sought to determine whether TeaA/TeaC and TeaC/SepA would interact. This was studied by BiFC. The N-terminal half of YFP (YFP^N) was fused to SepA and TeaA, and the C-terminal half of YFP (YFP^C) was tagged with TeaC. Strains expressing only YFP^N-SepA, YFP^N-TeaA, or YFP^C-TeaC showed no YFP fluorescence. In contrast, in the strain expressing both YFP^N-SepA and YFP^C-TeaC produced YFP signals as a single point and along the apex and at hyphal septa

TABLE 3. Localization pattern of mRFP1-TeaC[a]

Category	mRFP1-TeaC localization pattern (%)				
					
Wild type	72	3	13	13	2
Wild type with benomyl	19	0	6	4	71
Δ*kipA* mutant	44	33	4	18	1
KipA^{rigor} mutant	57	8	28	4	3
Wild type with cytochalasin A	25	5	7	13	50
Δ*teaA* mutant	0	4	0	2	94

[a] The localization pattern of mRFP1-TeaC of 100 to 200 hyphal tips was analyzed and grouped into six different categories. The construct was expressed from the *teaC* promoter. The numbers indicate the percentages of the hyphal tips of these groups. Hyphae were grown on minimal medium with glycerol as a carbon source for 1 day. For drug treatment, hyphae were incubated in the presence of 2.5 μg of benomyl/ml for 30 min or 2 μg of cytochalasin A/ml for 2 to 10 min.

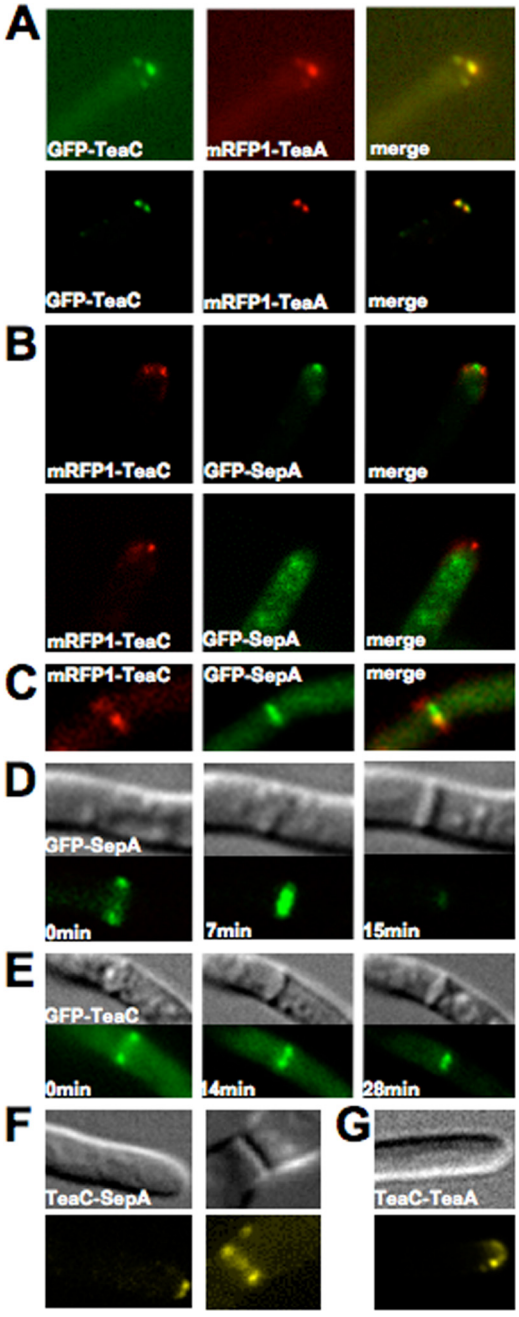

FIG. 7. Interaction of TeaC with TeaA and SepA. (A) Colocalization of TeaC and TeaA in strain SYH18; (B) visualization of TeaC and SepA in strain SYH13 at the hyphal tip; (C) partially colcalization of TeaC and SepA in strain SYH13 at the septa; (D) localization of SepA in strain SNT28; (E) localization of TeaC in strain SYH03; (F) interaction of TeaC with SepA (strain SYH05) shown in the bimolecular fluorescence complementation assay; (G) interaction of TeaC with TeaA (strain SYH06) shown in the bimolecular fluorescence complementation assay. Hyphae are 3 to 4 μm in diameter.

(Fig. 7F). In the case of the combination of YFP^N-TeaA and YFP^C-TeaC, YFP signals were detected only at the hyphal tip (Fig. 7G). We also tested YFP^N-TeaR (the membrane anchor protein) and YFP^C-TeaC interaction, but no YFP fluorescence was observed (data not shown). The observed interactions were analyzed with the yeast-two hybrid system. TeaA showed self-interaction and interaction with TeaC. In both cases, the C termini of TeaA and TeaC were important for the interaction (Fig. 8). Interaction of TeaC and SepA could not be detected in this assay, because SepA alone already induced the expression of the yeast two hybrid reporters (data not shown).

Localization dependency of TeaC and TeaA. We analyzed TeaC localization in a Δ*teaA* mutant and found that the correct positioning of TeaC depends on TeaA (Fig. 9A and Table 3). In the absence of TeaA, TeaC appeared dispersed in the cytoplasm. We also analyzed TeaA localization in a Δ*teaC* mutant. mRFP1-tagged TeaA did not concentrate in one point in the apex but appeared as several points along the membrane (Fig. 9B).

DISCUSSION

Polarized growth of *A. nidulans* is achieved through a collaborative action of the MT and the actin cytoskeleton, in which cell end marker proteins regulate polarity maintenance through the putative conserved mechanism of *S. pombe* (8). In the present study, we analyzed another component of the *S. pombe* machinery, the SH3-domain protein Tea4, which is involved in the transmission of positional information through the interaction with both Tea1 and the formin For3 (18). We show here that in *A. nidulans* TeaC serves functions in polarized growth and in septation. The role of TeaC will be discussed in the light of recent findings for *S. pombe* Tea4 and the closest *S. cerevisiae* homologue Bud14 (4, 15).

Deletion of *teaC* caused a growth defect and zig-zag hyphal phenotype, similar to but not identical to the one of the *teaA* deletion mutant. Interaction studies revealed that TeaC interacted with TeaA and SepA at hyphal tips. These results suggest that the function of TeaC at the hyphal tips is comparable to the function of Tea4 in *S. pombe*, namely, the recruitment of SepA to the growth zone and hence the polarization of the actin cytoskeleton. However, TeaC and SepA did not obviously colocalize at the hyphal tips, although protein-protein interaction was found. This may be explained by the mechanism of actin polymerization by formin. In *S. pombe*, it was suggested that For3 is activated and promotes actin filament assembly at the cell cortex for only a few seconds, and then For3 is inactivated and released from the cortex by retrograde flow along actin filaments (17). In *S. cerevisiae* it was shown recently that Bud14 displaces the formin from growing barbed ends of actin cables (4). On the other hand, it can also be that SepA is very dynamic at the tip and the interaction with TeaC is only weak and transient.

The zig-zag hyphal phenotype in the *teaC*-deletion mutant was weaker than that in the *teaA* deletion mutant, suggesting that the contribution of TeaC to the function for polarity maintenance is lower than that of TeaA. TeaA probably serves additional functions. In fact, in *S. pombe*, Tea1 is necessary for the localization of Pom1, a DYRK-family protein kinase (33). Pom1 kinase interacts with Rga4, which plays a role as GAP for Cdc42, a regulator of F-actin (32).

Besides the action of TeaC at the hyphal tip, we discovered that the protein localized at the septa. Similar to the situation at the hyphal tip, BiFC analysis showed the interaction between TeaC and SepA at septa, but TeaC did not obviously

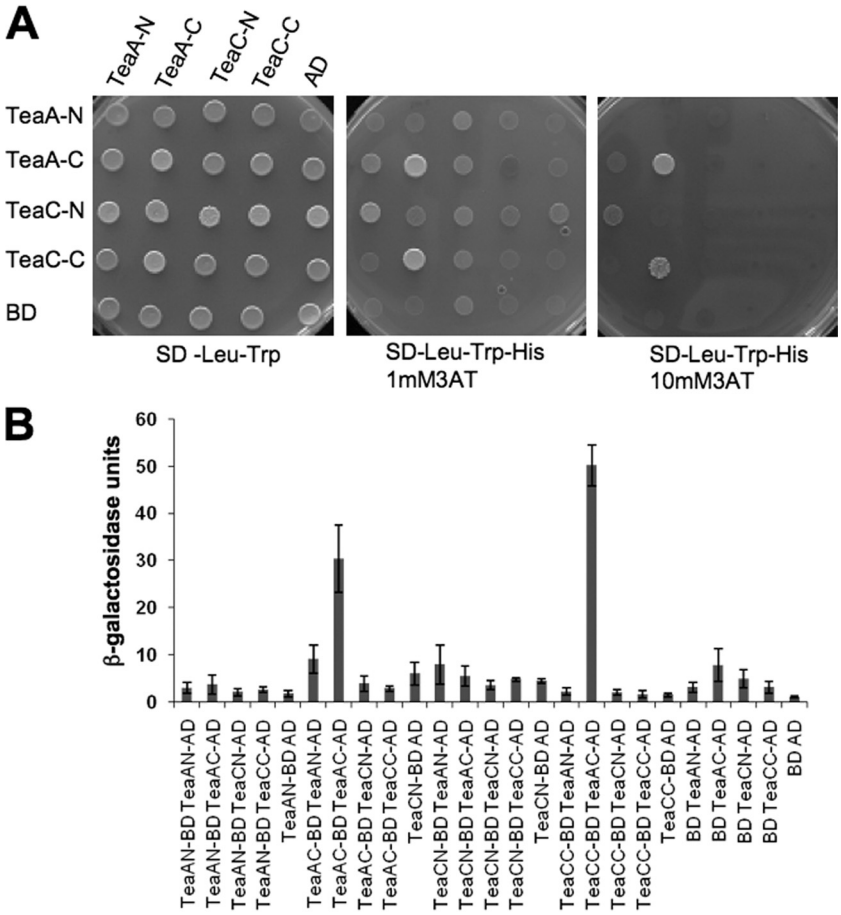

FIG. 8. Yeast two-hybrid assay to confirm the interactions described in Fig. 7. (A) Colonies of the yeast strains. The proteins indicated on the left side were fused to the binding domain (BD), and the proteins indicated above the picture were fused to the activation domain (AD). The mated yeasts were selected on SD−Leu−Trp plates and grown on SD medium (SD−Leu−Trp−His) supplemented with 1 mM or 10 mM 3AT (3-amino-1,2,4-triazole). (B) The β-galactosidase activity was analyzed from liquid cultures using ONPG as substrate and is expressed as Miller units. The data are expressed as the means of three independent experiments. The standard deviation is indicated.

colocalize with SepA. This may be explained again by the release of inactive formin from the plasma membrane at septation sites (17). The importance of TeaC at septa is also shown by our finding that overexpression of TeaC inhibits septation. However, in contrast to the role of SepA, TeaC appears not to be essential for septation, because deletion of *teaC* still allows normal septation (12a, 12b, 27a). There are several possibilities for how the inhibition effect can be explained. (i) Recently, it was shown that *S. cerevisiae* Bud14 negatively controls the activity of the formin Bni1 (4). If TeaC negatively controls SepA at septa, then overexpression would cause a reduction of the number of septa. Contradicting this idea is the finding that in *S. pombe* overexpression of Tea4 led to long actin cables (18). (ii) A large amount of TeaC protein in the cytoplasm could trap SepA in the cytoplasm and prevent specific localization at septation sites. In agreement with this hypothesis is the fact that we did not see any SepA-GFP rings when TeaC or TeaC and SepA were overexpressed and the germlings displayed in Fig. 4C observed in the GFP channel (data not shown). (iii) In *S. pombe*, the position of interphase nuclei determines the cleavage site through a protein called Mid1. Mid1 is a nuclear protein, which moves out of the nucleus upon phosphorylation and marks the cell cortex in the vicinity of the nucleus for septum formation (15, 21). Likewise, septation in *A. nidulans* depends on mitosis and the position of the nucleus (35, 36). However, as a difference to *S. pombe*,

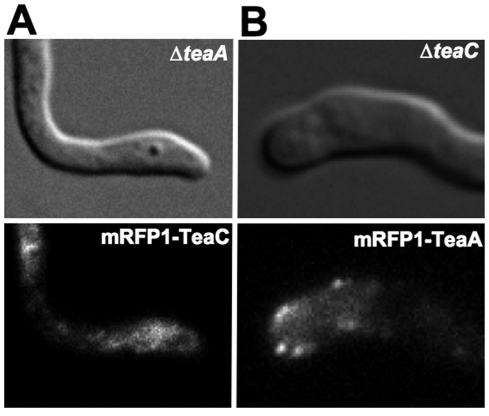

FIG. 9. Localization dependency of TeaC and TeaA. (A) TeaC localization in the Δ*teaA* mutant (SYH19); (B) TeaA localization in the Δ*teaC* mutant (SYH24). Hyphae are 3 to 4 μm in diameter.

septation does not follow every mitosis, with the result of multinucleate hyphal compartments (35). Given the importance of Mid1 for septum formation in *S. pombe*, we searched the *A. nidulans* genome for potential homologues but were unable to find one. Based on several examples, e.g., the cell end marker proteins are poorly conserved although they serve similar functions, we believe a Mid1 homologue could still exist in filamentous fungi. However, the activity of this postulated protein should be further regulated, because not all nuclear division planes are used for cytokinesis. TeaC might be involved in this selection by controlling the activity of a putative Mid1 homolgoue. Such a function for Tea4 has been shown recently as the mechanism for tip occlusion of septation in *S. pombe* (16). *teaC* deletion would thus impair site selection of septation. Indeed, we observed some short and empty compartments. Nevertheless, we did not find more septa close to the hyphal tip in *teaC* deletion strains, indicating that as-yet-unknown factors need to locally control the activity of a putative Mid1 homologue along the hyphae in addition to TeaC.

Another possibility to explain the role of TeaC in polarized growth and septation is the recruitment of other proteins involved in both processes. One candidate is the protein phosphatase 1 BimG, which is the *A. nidulans* homologue of *S. pombe* Dis2 and the *S. cerevisiae* homologue Glc7 (1, 10). This phosphatase localizes to different places in *A. nidulans*, among which is the membrane at growing tips and septa. The involvement in different processes, such as mitosis and hyphal growth, probably depends on several pathway-specific targets. Although there is evidence in *S. pombe* that Tea4 interacts with Dis2, and the localization pattern of TeaC at the septum resembles the pattern of BimG, the localization pattern of the two proteins at the tip looks different. Whereas BimG localizes along the membrane and excludes the very tip, TeaC appears to be restricted to the very tip. Therefore, a direct link to TeaC remains to be shown.

ACKNOWLEDGMENTS

This study was supported by the priority program "Lebensmittel und Gesundheit" of the Landesstiftung Baden Württemberg, by the Center for Functional Nanostructures, and by the DFG. N.T. was a fellow of the Humboldt Foundation.

REFERENCES

1. **Alvarez-Tabarés, I., A. Grallert, J. M. Ortiz, and I. M. Hagan.** 2007. *Schizosaccharomyces pombe* protein phosphatase 1 in mitosis, endocytosis and a partnership with Wsh3/Tea4 to control polarized growth. J. Cell Sci. **120:** 3589–3601.
2. **Basu, R., and F. Chang.** 2007. Shaping the actin cytoskeleton using microtubule tips. Curr. Opin. Cell Biol. **19:**1–7.
3. **Browning, H., D. D. Hackney, and P. Nurse.** 2003. Targeted movement of cell end factors in fission yeast. Nat. Cell Biol. **5:**812–818.
4. **Chesarone, M., C. J. Gould, J. B. Moseley, and B. L. Goode.** 2009. Displacement of formins from growing barbed ends by Bud14 is critical for actin cable architecture and function. Dev. Cell **16:**202–302.
5. **Efimov, V., J. Zhang, and X. Xiang.** 2006. CLIP-170 homologue and NUDE play overlapping roles in NUDF localization in *Aspergillus nidulans*. Mol. Biol. Cell **17:**2021–2034.
6. **Enke, C., N. Zekert, D. Veith, C. Schaaf, S. Konzack, and R. Fischer.** 2007. *Aspergillus nidulans* Dis1/XMAP215 protein AlpA localizes to spindle pole bodies and microtubule plus ends and contributes to growth directionality. Eukaryot. Cell **6:**555–562.
7. **Feierbach, G., F. Verde, and F. Chang.** 2004. Regulation of a formin complex by the microtubule plus end protein tea1p. J. Cell Biol. **165:**697–707.
8. **Fischer, R., N. Zekert, and N. Takeshita.** 2008. Polarized growth in fungi: interplay between the cytoskeleton, positional markers, and membrane domains. Mol. Microbiol. **68:**813–826.
9. **Fischer-Parton, S., R. M. Parton, P. C. Hickey, J. Dijksterhuis, H. A. Atkinson, and N. D. Read.** 2000. Confocal microscopy of FM4-64 as a tool for analyzing endocytosis and vesicle trafficking in living fungal hyphae. J. Microsc. **198:**246–259.
10. **Fox, H., P. C. Hickey, J. M. Fernández-Ábalos, P. Lunness, N. D. Read, and J. H. Doonan.** 2002. Dynamic distribution of BIMG^{PP1} in living hyphae of *Aspergillus* indicates a novel role in septum formation. Mol. Microbiol. **45:** 1219–1230.
11. **Galagan, J. E., S. E. Calvo, C. Cuomo, L.-J. Ma, J. R. Wortman, S. Batzoglou, S.-I. Lee, M. Bastürkmen, C. C. Spevak, J. Clutterbuck, V. Kapitonov, J. Jurka, C. Scazzocchio, M. Farman, J. Butler, S. Purcell, S. Harris, G. H. Braus, O. Draht, S. Busch, C. d'Enfert, C. Bouchier, G. H. Goldman, D. Bell-Pedersen, S. Griffiths-Jones, J. H. Doonan, J. Yu, K. Vienken, A. Pain, M. Freitag, E. U. Selker, D. B. Archer, M. A. Peñalva, B. R. Oakley, M. Momany, T. Tanaka, T. Kumagai, K. Asai, M. Machida, W. C. Nierman, D. W. Denning, M. Caddick, M. Hynes, M. Paoletti, R. Fischer, B. Miller, P. Dyer, M. S. Sachs, S. A. Osmani, and B. W. Birren.** 2005. Sequencing of *Aspergillus nidulans* and comparative analysis with *A. fumigatus* and *A. oryzae*. Nature **438:**1105–1115.
12. **Harris, S. D., N. D. Read, R. W. Roberson, B. Shaw, S. Seiler, M. Plamann, and M. Momany.** 2005. Polarisome meets Spitzenkörper: microscopy, genetics, and genomics converge. Eukaryot. Cell **4:**225–229.

12a. **Harris, S. D., L. Hamer, K. E. Sharpless, and J. E. Hamer.** 1997. The *Aspergillus nidulans sepA* gene encodes an FH1/2 protein involved in cytokinesis and the maintenance of cellular polarity. EMBO J. **16:**3474–3483.

12b. **Harris, S. D., J. L. Morrell, and J. E. Hamer.** 1994. Identification and characterization of *Aspergillus nidulans* mutants defective in cytokinesis. Genetics **136:**517–532.

13. **Hill, T. W., and E. Käfer.** 2001. Improved protocols for *Aspergillus* minimal medium: trace element and minimal medium salt stock solutions. Fungal Genet. Newsl. **48:**20–21.
14. **Horio, T., and B. R. Oakley.** 2005. The role of microtubules in rapid hyphal tip growth of *Aspergillus nidulans*. Mol. Biol. Cell **16:**918–926.
15. **Huang, Y., T. G. Chew, W. Ge, and M. K. Balasubramanian.** 2007. Polarity determinants Tea1p, Tea4p, and Pom1p inhibit division-septum assembly at cell end in fission yeast. Dev. Cell **12:**987–996.
16. **Konzack, S., P. Rischitor, C. Enke, and R. Fischer.** 2005. The role of the kinesin motor KipA in microtubule organization and polarized growth of *Aspergillus nidulans*. Mol. Biol. Cell **16:**497–506.
17. **Martin, S. G., and F. Chang.** 2006. Dynamics of the formin for3p in actin cable assembly. Curr. Biol. **16:**1161–1170.
18. **Martin, S. G., W. H. McDonald, J. R. r. Yates, and F. Chang.** 2005. Tea4p links microtubule plus ends with the formin for3p in the establishment of cell polarity. Dev. Cell **8:**479–491.
19. **Mata, J., and P. Nurse.** 1997. tea1 and the microtubular cytoskeleton are important for generating global spatial order within the fission yeast cell. Cell **89:**939–949.
20. **Miller, J. H.** 1972. Experiments in molecular genetics. Cold Spring Harbor Laboratory Press, Cold Spring Harbor, NY.
21. **Motegi, F., M. Mishra, M. K. Balasubramanian, and I. Mabuchi.** 2004. Myosin-II reorganization during mitosis is controlled temporally by its dephosphorylation and spatially by Mid1 in fission yeast. J. Cell Biol. **265:**685–695.
22. **Nayak, T., E. Szewczyk, C. E. Oakley, A. Osmani, L. Ukil, S. L. Murray, M. J. Hynes, S. A. Osmani, and B. R. Oakley.** 2006. A versatile and efficient gene targeting system for *Aspergillus nidulans*. Genetics **172:**1557–1566.
23. **Peñalva, M. A.** 2005. Tracing the endocytic pathway of *Aspergillus nidulans* with FM4-64. Fungal Genet. Biol. **42:**963–975.
24. **Riquelme, M., S. Bartnicki-Garcia, J. M. González-Prieto, E. Sánchez-León, J. A. Verdín-Ramos, A. Beltrán-Aguilar, and M. Freitag.** 2007. Spitzenkorper localization and intracellular traffic of green fluorescent protein-labeled CHS-3 and CHS-6 chitin synthases in living hyphae of *Neurospora crassa*. Eukaryot. Cell **6:**1853–1864.
25. **Riquelme, M., C. G. Reynaga-Peña, G. Gierz, and S. Bartnicki-García.** 1998. What determines growth direction in fungal hyphae? Fungal Genet. Biol. **24:**101–109.
26. **Sambrook, J., and D. W. Russell.** 1999. Molecular cloning: a laboratory manual. Cold Spring Harbor Laboratory Press, Cold Spring Harbor, NY.
27. **Sampson, K., and I. B. Heath.** 2005. The dynamic behavior of microtubules and their contributions to hyphal tip growth in *Aspergillus nidulans*. Microbiology **151:**1543–1555.

27a. **Sharpless, K. E., and S. D. Harris.** 2002. Functional characterization and localization of the *Aspergillus nidulans*. forming SEPA. Mol. Biol. Cell **13:** 469–479.

28. **Snaith, H. A., and K. E. Sawin.** 2003. Fission yeast mod5p regulates polarized growth through anchoring of tea1p at cell tips. Nature **423:**647–651.
29. **Snell, V., and P. Nurse.** 1994. Genetic analysis of cell morphogenesis in fission yeast: a role for casein kinase II in the establishment of polarized growth. EMBO J. **13:**2066–2074.
30. **Stringer, M. A., R. A. Dean, T. C. Sewall, and W. E. Timberlake.** 1991. Rodletless, a new *Aspergillus* developmental mutant induced by directed gene inactivation. Genes Dev. **5:**1161–1171.

30a. **Taheri-Talesh, N., T. Horio, L. Araujo-Bazan, X. Dou, E. A. Espeso, M. A.**

Penalva, A. Osmani, and B. R. Oakley. 2008. The tip growth apparatus of *Aspergillus nidulans*. Mol. Biol. Cell **19:**1439–1449.
31. **Takeshita, N., Y. Higashitsuji, S. Konzack, and R. Fischer.** 2008. Apical sterol-rich membranes are essential for localizing cell end markers that determine growth directionality in the filamentous fungus *Aspergillus nidulans*. Mol. Biol. Cell **19:**339–351.
32. **Tatebe, H., K. Nakano, R. Maximo, and K. Shiozaki.** 2008. Pom1 DYRK regulates localization of the Rga4 GAP to ensure bipolar activation of Cdc42 in fission yeast. Curr. Biol. **18:**322–330.
33. **Tatebe, H., K. Shimada, S. Uzawa, S. Morigasaki, and K. Shiozaki.** 2005. Wsh3/Tea4 is a novel cell-end factor essential for bipolar distribution of Tea1 and protects cell polarity under environmental stress in *Schizosaccharomyces pombe*. Curr. Biol. **15:**1006–1015.
34. **Veith, D., N. Scherr, V. P. Efimov, and R. Fischer.** 2005. Role of the spindle-pole body protein ApsB and the cortex protein ApsA in microtubule organization and nuclear migration in *Aspergillus nidulans*. J. Cell Sci. **118:**3705–3716.
35. **Wolkow, T. D., S. D. Harris, and J. E. Hamer.** 1996. Cytokinesis in *Aspergillus nidulans* is controlled by cell size, nuclear positioning and mitosis. J. Cell Sci. **109:**2179–2188.
36. **Xiang, X., S. M. Beckwith, and N. R. Morris.** 1994. Cytoplasmic dynein is involved in nuclear migration in *Aspergillus nidulans*. Proc. Natl. Acad. Sci. USA **91:**2100–2104.
37. **Yelton, M. M., J. E. Hamer, and W. E. Timberlake.** 1984. Transformation of *Aspergillus nidulans* by using a trpC plasmid. Proc. Natl. Acad. Sci. USA **81:**1470–1474.
38. **Zekert, N., and R. Fischer.** 2009. The *Aspergillus nidulans* kinesin-3 UncA motor moves vesicles along a subpopulation of microtubules. Mol. Biol. Cell **20:**673–684.